

Metal enhanced fluorescence in rare earth doped plasmonic core-shell nanoparticles

S. Derom¹, A. Berthelot², A. Pillonnet², O. Benamara², A.M. Jurdyc², C. Girard³ and G. Colas des Francs¹

¹Laboratoire Interdisciplinaire Carnot de Bourgogne (ICB), UMR 6303 CNRS-Université de Bourgogne, 9 Av. A. Savary, BP 47 870, F-21078 Dijon, France

²Institut Lumière Matière, UMR 5306 Université de Lyon 1-CNRS, Université Lyon, Villeurbanne F-69622, France

³Centre d'Elaboration de Matériaux et d'Etudes Structurales (CEMES), CNRS, 29 rue J. Marvig, BP 94347, F-31055 Toulouse Cedex 4, France

E-mail: gerard.colas-des-francs@u-bourgogne.fr

Submitted to: *Nanotechnology*

Abstract. We theoretically and numerically investigate metal enhanced fluorescence of plasmonic core-shell nanoparticles doped with rare earth (RE) ions. Particle shape and size are engineered to maximize the average enhancement factor (AEF) of the overall doped shell. We show that the highest enhancement (11 in the visible and 7 in the near-infrared) are achieved by tuning either the dipolar or quadrupolar particle resonance to the rare earth ions excitation wavelength. Additionally, the calculated AEFs are compared to experimental data reported in the literature, obtained in similar conditions (plasmon mediated enhancement) or when a metal-RE energy transfer mechanism is involved.

1. Introduction

Rare earth (RE) ions are widely studied for numerous optical applications such as solar cells [1], optical amplification, biolabelling [2] but also photodynamic therapy of cancer [3]. Although they present high quantum efficiencies, they could suffer from low absorption cross-section [4] (around 10^{-20}cm^2) so that metal enhanced fluorescence (MEF) has been proposed to improve their emission properties.

Metal enhanced spectroscopies rely on the excitation and/or emission exaltation by coupling emitters to a plasmonic particle. This has been extensively studied, notably for Tip- or Surface- Enhanced Raman Scattering (TERS/SERS) [5] or dye fluorescence enhancement [6, 7]. Practically, the highest signal enhancement is achieved for low initial absorption cross-section *and* quantum yield, since both excitation and emissions processes are enhanced. Sun *et al* described SERS as photoluminescence enhancement in the limit of null initial absorption cross section and quantum yield [8]. Therefore, SERS presents the highest enhancement (up to 10^6) [9] whereas MEF is typically of few tens only [10]. Nevertheless, the results achieved for dye molecules cannot be directly transposed to rare-earth ions which present extremelly low absorption cross-section but quantum efficiency close to unity on the contrary to dyes which present high absorption cross-section, and generally lower quantum efficiency. In addition, it is worthwhile to note that lanthanides luminescence is also extremelly sensitive to the surroundings so that identifying the role of plasmon is a difficult task.

A large number of works, mainly experimental [11, 12, 13, 14, 15, 16, 17, 18, 19, 20, 21, 22], but also theoretical [23, 24, 25], have been realized in order to probe the possibility to enhance optical properties of rare earth ions placed near metal nanoparticles. Some recent works have highlighted that gold or silver metal nanoparticle could change the selection rules of rare earth ions emission [16, 26] but the localized plasmon contribution remains in discussion. Indeed, it is very difficult to separate respective roles of plasmon and energy transfer in the observed enhancement of RE ions luminescence [27]. Plasmon mediated enhancement relies on antenna effect that increases the excitation field and/or radiative emission rate [28], whereas energy transfer is a dipole-dipole Förster-like mechanism between the metal nanocrystal (donor or sensitizer) and RE ions (acceptor) [11]. It has been observed that energy transfer is at the origin of luminescence enhancement near small gold and silver clusters composed by few atoms (crystal size of few nm) [27, 29]. However, larger metal particles (typically few tens of nm) are generally preferred for plasmon-enhanced fluorescence [14, 18, 19, 20, 22]. Recently, Ma *et al* measured 3-fold and 24-fold enhancement factor for Eu^{3+} doped silver core-shell nanoparticles with 20 nm core/15 nm shell and 9 nm core/11 nm shell, respectively [15]. However, they used $\lambda_{exc} = 260$ nm excitation wavelength far from the dipolar resonance so that we think that the enhancement mechanism is different from plasmon enhanced spectroscopy and most likely originates from energy transfer. Two others groups reported 3 fold enhancement for Eu^{3+} ions coupled to about 30 nm silver particles when excited close to the silver dipolar resonance [19, 22]. In a

former work, Malta and Couto dos Santos have made a rough estimation of the possible emission enhancement for Europium ions doped glasses containing silver nanoparticles [23]. They estimated up to 50-fold maximum *local* enhancement factor for 30 nm silver particles but not conclude about the global enhancement of the overall doped shell.

The purpose of this work is to theoretically determine and optimize the plasmon contribution to the luminescence enhancement in plasmonic nanoparticle doped with lanthanides. Particular attention is devoted to describe an ensemble of rare earth ions coupled to a metallic nanoparticle instead of single emitter coupled to one particle as generally done since we are interested in the optical response of the whole doped nanostructure. In a first time, we investigate the role of the localized plasmons supported by the nanoparticle and determine the optimal particle resonance position compared to the emitter absorption and emission peak. To this end, we define in section 2, the average fluorescence factor for a doped plasmonic core-shell particle of arbitrary shape. For comparison purpose, we illustrate the enhancement mechanism by considering a laser dye, namely the Rhodamine 6G (Rh6G) coupled to a spherical metal particle [30]. In a second time, in section 3, we investigate the fluorescence enhancement for rare earth ions emitting in the visible or the near infrared and placed in the shell of core-shell particles with metal core. We will thus estimate the achievable plasmonic enhancement.

2. Surface enhanced fluorescence

In this section, we derive a general expression for the average fluorescent enhancement factor (AEF) near a metal particle. To this aim, we extend the work of Liaw *et al* [31] to an arbitrary geometry. We first derive a closed form expression of the enhancement factor $\alpha(\mathbf{r})$ for randomly oriented emitters near a metal particle. AEF is then achieved by numerically averaging $\alpha(\mathbf{r})$ over the doped shell volume.

2.1. Enhancement factor of randomly oriented emitters

Let us first consider a single fluorescent system with a transition dipolar moment of arbitrary orientation $\mathbf{p} = p_0(\sin \alpha \cos \beta, \sin \alpha \sin \beta, \cos \alpha)$ and intrinsic quantum yield η_0 . If the incident field is \mathbf{E}_0 , the fluorescent signal in absence of plasmonic particle is $p_0^2 |\mathbf{E}_0|^2 \eta_0$. The plasmonic particle modifies:

- the excitation rate $\pi(\mathbf{r}, \omega_{exc}) = |\mathbf{p} \cdot \mathbf{E}(\mathbf{r}, \omega_{exc})|^2 / p_0^2 |\mathbf{E}_0|^2$ where $\mathbf{E}(\mathbf{r}, \omega_{exc})$ refers to the excitation field at the emitter location \mathbf{r} and excitation angular frequency ω_{exc}
- and the emitter quantum yield $\eta(\mathbf{r}, \omega_{em}) = \gamma^{rad} / (\gamma^{rad} + \gamma^{NR})$ at the emission angular frequency ω_{em} .

As an example, we present on Fig. 1 the excitation and decay rates calculated for an emitter close to gold or silver beads. The emitter is perpendicular to the particle surface since stronger effects are expected for this orientation. The excitation and radiative rates follow the dipolar plasmon mode dispersion for small particle diameters. Large particles

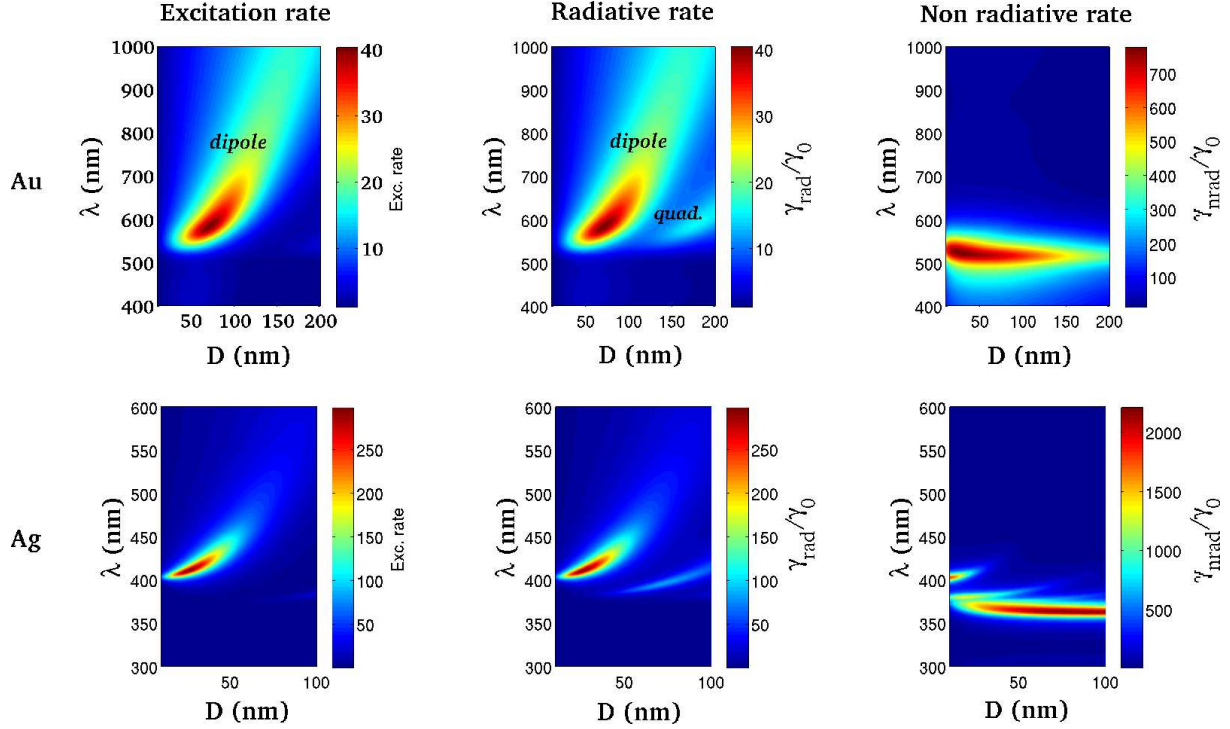


Figure 1. Excitation (left), radiative (middle) and non-radiative (right) rates near a metal spherical particle as a function of wavelength and particle diameter D . Top (bottom) line refers to gold (silver) particle. The dipolar emitter is located 5 nm from the particle surface and perpendicular to it. The optical index of the embedding matrix is $n=1.5$. Metal dielectric constant are taken from Johnson and Christy [32].

support a leaky quadrupolar mode so that the radiative rate couples to this mode. Note that the excitation rate weakly follows the quadrupolar mode dispersion since the emitter is not located on a mode lobe. Finally, the non radiative rate originates from coupling to high order modes so that it presents a flat dispersion curve [33]. The low order modes are well-separated in case of a silver particle due to lower losses (compare the non radiative rate near gold and silver structures). Last, we observe that the dipolar plasmon resonance can be tuned from $\lambda = 525$ nm (well-defined resonance) to $\lambda \approx 900$ nm (large resonance) for gold beads diameters varying from $D = 10$ nm to $D = 200$ nm. For silver nanoparticles diameters between 10 nm and 100 nm, the dipolar resonance wavelength varies from $\lambda = 400$ nm to $\lambda = 530$ nm.

Finally, both the excitation and emission rates depend on the emitter location and orientation in presence of plasmonic nanostructures. The enhancement factor expresses

$$\alpha_{\mathbf{p}}(\mathbf{r}, \omega_{exc}, \omega_{em}) = \frac{|\mathbf{p} \cdot \mathbf{E}(\mathbf{r}, \omega_{exc})|^2 \eta(\mathbf{r}, \omega_{em})}{p_0^2 |\mathbf{E}_0|^2 \eta_0}. \quad (1)$$

In case of arbitrary orientation, the quantum yield expresses [34]

$$\begin{aligned} \eta = & \sin^2 \alpha \cos^2 \beta \eta_x + \sin^2 \alpha \sin^2 \beta \eta_y + \cos^2 \alpha \eta_z \\ & + \sin^2 \alpha \cos \beta \sin \beta \eta_{xy} + \sin \alpha \cos \alpha \cos \beta \eta_{xz} + \sin \alpha \cos \alpha \sin \beta \eta_{yz}, \end{aligned} \quad (2)$$

where $\eta_i = \Gamma_{rad,i}/(\Gamma_{rad,i} + \Gamma_{NR,i})$ is the quantum yield associated to the i -orientation ($i=x,y$ or z). η_{ij} ($i,j=x,y$ or z) refer to crossed-terms that have to be considered for oblique dipole moments (see Refs. [34, 35] for details). Assuming randomly oriented emitters at location \mathbf{r} , we calculate the mean enhancement factor over all the possible orientations

$$\alpha(\mathbf{r}, \omega_{exc}, \omega_{em}) = \frac{3}{4\pi} \int_{\alpha=0}^{\pi} \int_{\beta=0}^{2\pi} \alpha_{\mathbf{p}}(\mathbf{r}, \omega_{exc}, \omega_{em}) \sin \alpha \, d\alpha \, d\beta, \quad (3)$$

where the factor 3 ensures a unit enhancement factor for isolated emitters excited with a linearly polarized field. Interestingly enough, the integration over the dipole orientation is analytical. After a few algebra, we achieve

$$\begin{aligned} \alpha(\mathbf{r}, \omega_{exc}, \omega_{em}) &= \\ &= \frac{\eta_x(3E_x^2 + E_y^2 + E_z^2) + \eta_y(E_x^2 + 3E_y^2 + E_z^2) + \eta_z(E_x^2 + E_y^2 + 3E_z^2)}{5 |\mathbf{E}_0|^2 \eta_0}. \end{aligned} \quad (4)$$

It is also useful to derive this expression in spherical coordinates $\mathbf{r} = (r, \theta, \phi)$. With subscripts $//$ and \perp indicating an orientation parallel or perpendicular to the particle surface, it writes

$$\alpha(\mathbf{r}, \omega_{exc}, \omega_{em}) = \frac{\eta_{//}(2E_r^2 + 4E_\theta^2 + 4E_\phi^2) + \eta_\perp(3E_r^2 + E_\theta^2 + E_\phi^2)}{5 |\mathbf{E}_0|^2 \eta_0}, \quad (5)$$

that leads to an analytical expression for (homogeneous, core-shell or onion-like) spherical particles, thanks to Mie expansion [36, 37]. In the following, $\alpha(\mathbf{r}, \omega_{exc}, \omega_{em})$ is referred as the local fluorescence enhancement.

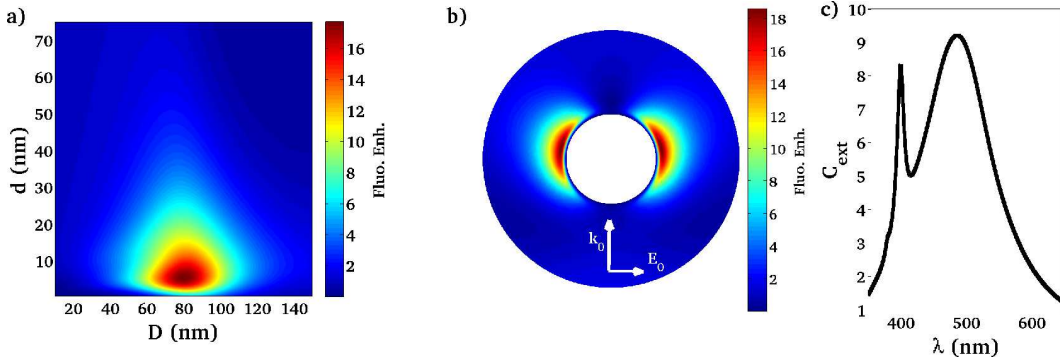


Figure 2. Fluorescence enhancement near a silver particle for randomly oriented molecules. a) As a function of the particle diameter and dye-particle distance (the molecules are along the incident field polarization axis). b) Near a 80 nm silver particle. The excitation and emission wavelength are $\lambda_{exc} = 532\text{nm}$ and $\lambda_{em} = 560\text{nm}$, respectively. The embedding medium is PMMA (optical index $n = 1.5$). c) Extinction efficiency of a 80 nm silver particle.

Obviously, the choice of the particle size, shape and material depends on the fluorescent system. In case of dye molecules, with a low Stokes shift between the absorption and emission wavelength, the most efficient fluorescent enhancement is

achieved when the particle dipolar resonance overlaps both the excitation and emission wavelengths [10, 38]. For instance, let us consider Rhodamine 6G. We will compare rare-earth doped nanoparticle to this reference system. The absorption and emission peaks are near $\lambda_{exc} = 532$ nm and $\lambda_{em} = 560$ nm, respectively. Figure 2 shows the local fluorescent enhancement for randomly oriented Rh6G molecules dispersed in polymethyl metacrylate (PMMA) near silver spherical particles. The maximum fluorescence enhancement occurs for dye molecules coupled to a 80 nm particle (Fig. 2a). Such large silver bead support a dipolar plasmon about $\lambda \approx 500$ nm with a broad resonance width (and a quadrupolar mode at $\lambda = 400$ nm, see Fig.2c). Therefore both excitation field and radiative rates are significantly enhanced by coupling to the dipolar mode. Meanwhile, the non-radiative rate remains limited due to bad coupling to high order modes that appear at lower wavelength (see also Fig. 1). Figure 2b) presents the local enhancement factor calculated near a 80 nm silver sphere. It follows the particle dipolar mode profile, with a maximum enhancement $\alpha \approx 18$ slightly shifted from the incident polarisation axis [31, 39].

2.2. Layer- and shell-average enhancement factor

Finally, the average enhancement factor of the whole doped volume V_0 can be numerically computed as

$$AEF(\omega_{exc}, \omega_{em}) = \frac{1}{V_0} \iiint_{\mathbf{r} \in V_0} \alpha(\mathbf{r}, \omega_{exc}, \omega_{em}) dV \quad (6)$$

In case of spherical particles, it is also useful to define an average enhancement factor associated to a doped shell layer

$$\alpha_{layer}(\omega_{exc}, \omega_{em}, \mathbf{r}) = \frac{1}{4\pi} \int_{\theta=0}^{\pi} \int_{\phi=0}^{2\pi} \alpha(\mathbf{r}, \omega_{exc}, \omega_{em}) \sin \theta d\theta d\phi \quad (7)$$

Note that average and layer fluorescence enhancement factors are normalized with respect to the doped volume so that they do not depend on the RE concentration but rather characterize the SPP mediated fluorescence enhancement.

Figure 3 shows the layer fluorescence enhancement α_{layer} and the average fluorescence factor of the dye doped core-shell particle. The overall $AEF \approx 4$ is optimized given the absorption and emission wavelengths of the dye molecule. This factor takes into account inhomogeneous excitation in the dipolar modes as well as the distance dependence of the emission rate.

3. Rare earth doped plasmonic core shell

In the previous section, we have introduced two important parameters in order to quantify plasmon/emitters interactions in a core-shell particle: layer-averaged enhancement factor α_{layer} , and shell-averaged enhancement factor AEF. We have estimated maximum $AEF \approx 4$ achievable for a Rh6G doped core-shell Ag@SiO₂

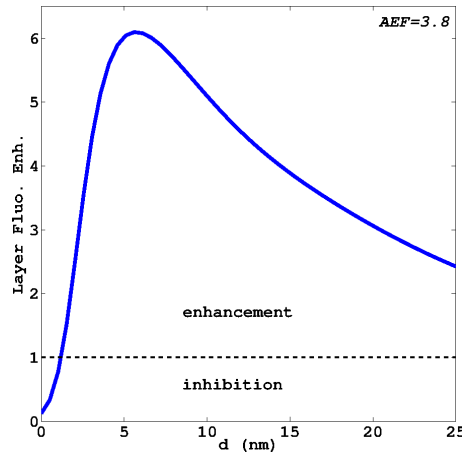


Figure 3. Layer fluorescence enhancement of a Rh6G doped core-shell Ag@SiO₂ (silver core 80 nm diameter). The horizontal line indicates the enhancement/inhibition threshold. The average fluorescence enhancement of the whole doped layer (25 nm) is $AEF = 3.8$.

reference system. These factors will now allow us to characterize the effect of a metal nanoparticle on the luminescence of RE ions.

In this part, we study the luminescence enhancement for two rare earth ions used in different application domains: Eu³⁺ used for example as biolabel for its emission in the visible spectrum and Er³⁺, as main active medium for amplification at the telecom wavelength 1.55 μm . Compared to the dye case, the situation could be rather different when considering rare earth ions fluorescence. Quantum efficiency of these emitters is close to unity, so plasmon resonance cannot much increase this factor. Lanthanide absorption, based on 4f transitions, in contrast, is very weak (around $10^{-20} cm^2$). Therefore, the strongest exaltation is expected when matching the lanthanide absorption wavelength with the dipolar plasmon resonance. Emission of lanthanide could be far from excitation wavelength and then probably not much influenced by plasmon phenomenon [40] contrary to previous section where the dye excitation and emission peaks were within the dipolar resonance.

3.1. Emission in the visible

First we consider Europium system: this rare earth ion, usually UV/blue excited, has a maximum emission around 620 nm and a quantum yield close to 1. Since their excitation corresponding to 5D₀-7F₂ transition is in the blue part of the visible spectrum, we have chosen to use silver for the nanoparticle core.

We investigate Eu³⁺/silver system in Fig. 4, where rare earth ions (Eu³⁺) are included in a dielectric shell and coupled to a silver bead. We consider a silica matrix of same index as PMMA so that direct comparison with the previous dye molecule case is possible. This luminescent doped core-shell Ag@SiO₂ particle can be chemically synthesized [14, 18, 20]. The excitation and emission wavelengths are $\lambda_{exc} = 415$ nm and

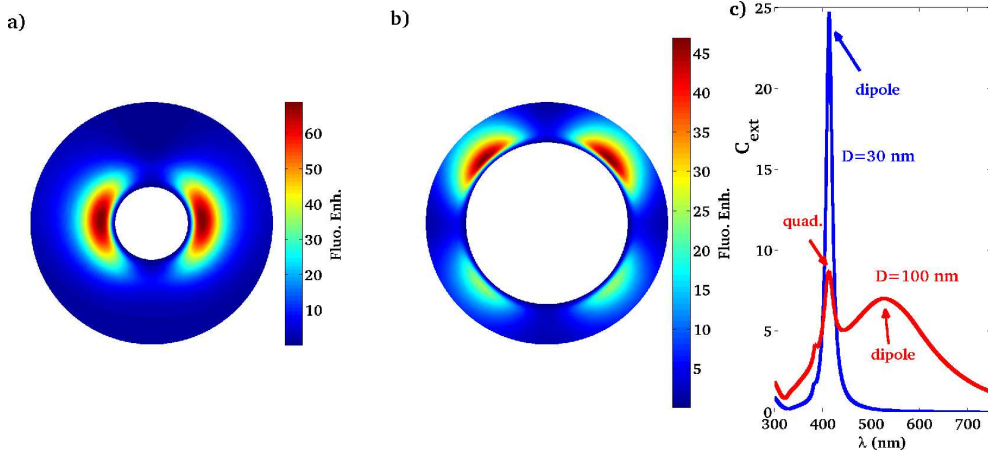


Figure 4. Eu^{3+} fluorescence enhancement near a 30 nm (a) or 100 nm (b) silver particle. c) Extinction efficiency of a 30 nm (blue line) or 100 nm (red line) silver particle. The dipolar and quadrupolar resonance are indicated for the two particle diameters. Excitation and emission wavelength are $\lambda_{exc} = 415$ nm and $\lambda_{em} = 620$ nm, respectively. The embedding medium is SiO_2 (optical index $n = 1.5$).

	d	exc. rate	γ_{rad}/γ_0	γ_{NR}/γ_0	η	flu. enh.	AEF
Rh6G- $\text{Ag}(80 \text{ nm})@\text{SiO}_2$	4 nm	35	9.7	5	0.66	19	3.8
Eu^{3+} - $\text{Ag}(30 \text{ nm})@\text{SiO}_2$	6 nm	210	1.8	3	0.37	69	11.0
Eu^{3+} - $\text{Ag}(100 \text{ nm})@\text{SiO}_2$	5.5 nm	90	8.	4.2	0.66	47	6.7

Table 1. Comparison of excitation and emission rates modification calculated at the optimum distance for Rh6G and Eu^{3+} doped silver core-shell. The local fluorescence enhancement is slightly below the product of excitation rate \times apparent quantum yield since it obeys to Eq.5.

$\lambda_{em} = 620$ nm, respectively, corresponding to f-f intra-configurational transitions. As previously, we first determine the size of the metal core that optimizes red luminescence of the europium ions. We find that the maximum local fluorescent enhancement (≈ 70) is obtained for a 30 nm silver core. We plot in Fig. 4a the map of the fluorescence exaltation achieved near the 30 nm silver sphere. This enhancement is mainly an improvement of absorption process: we have a strong exaltation of the excitation field resonant with the dipolar resonance of metal nanoparticle. Since the emission wavelength is far from all the particle resonances (see the extinction efficiency in Fig. 4c), decay rates are practically not affected by the presence of the plasmonic nanostructure. Table 1 gathers the excitation and decay rates for dye-doped and RE-doped silver core-shell. For dye molecules, with small Stokes shifts, large particles leads to stronger effect since it corresponds to large resonances and coupling to the dipolar plasmon enhances both the excitation and radiative emission rates. Differently, particles with small metal cores are better candidates to enhance RE emission. This leads to a strong excitation rate increase that compensates the decrease of the apparent quantum yield.

By increasing metal nanoparticle size, we observe a second optimum size (100

nm) for which efficient exaltation of the europium fluorescent signal occurs (≈ 50) (Fig. 4b). In this later case, the excitation field couples to the plasmon quadrupolar mode ($\lambda = 415$ nm) and radiative rate is also efficiently enhanced by coupling to the dipolar mode ($\lambda \approx 525$ nm, Fig. 4c). This leads to intermediate luminescence enhancement as compared to dye-doped system and dipolar assisted RE luminescence enhancement (see table 1). In addition, this possibility to enhance the excitation by coupling to the quadrupolar quadrupolar and emission by coupling to the dipolar resonance offers a supplementary degree of freedom for luminescence control.

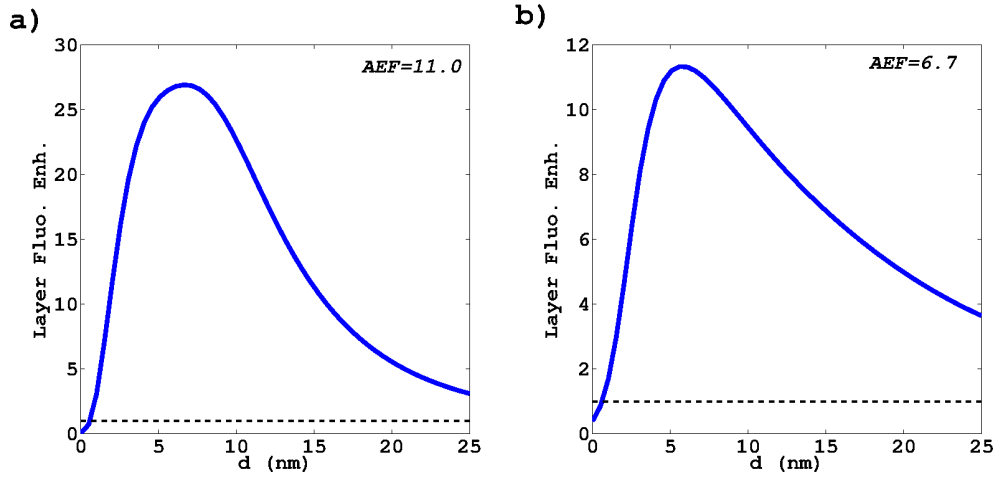


Figure 5. Layer fluorescence enhancement of a Eu^{3+} doped core-shell $\text{Ag}@\text{SiO}_2$ spherical particle. with a silver core of 30 nm (a) or 100 nm (b). The average fluorescence enhancement of the whole doped layer (25 nm) is reported on each figure. The horizontal line indicates the enhancement/inhibition threshold.

Having determined the optimal nanoparticle sizes in order to enhance red luminescent of a single Eu^{3+} ion, we now estimate the enhancement of an infinitely thin doped shell. Figure 5 shows the evolution of the layer fluorescence enhancement α_{layer} with distance between metal and emitters and the average fluorescence enhancement factor for the whole Eu^{3+} doped shell for these two optimal sizes. For a metal core 30 nm and doped shell thickness of 25 nm, we achieve a strong $AEF = 11$. This high AEF relies on the strong field enhancement at the plasmon dipolar mode resonance. Quenching is limited to emitters very close to the metal surface.

Finally, it is not possible to achieve fluorescence enhancement for these rare earth doped systems using a gold core (even optimizing the core diameter) since the gold particle dipolar resonance cannot be tuned to the Eu^{3+} absorption peak $\lambda = 415$ nm (see Fig. 1).

3.2. Emission in the near infrared

3.2.1. Spherical core-shell particle Erbium ions (Er^{3+}) are widely used for optical amplification for telecom applications since they emit around $\lambda_{em} = 1.55 \mu\text{m}$.

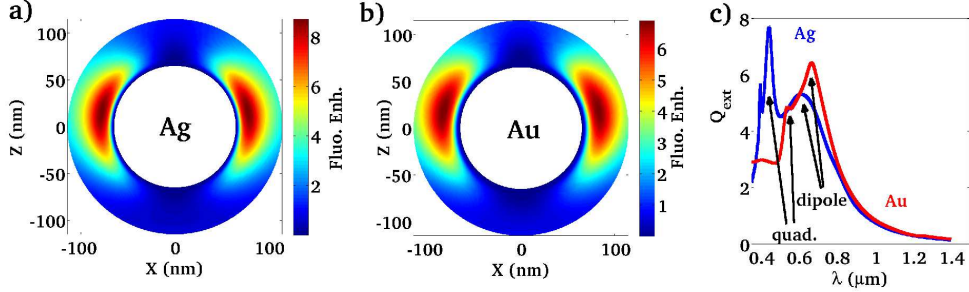


Figure 6. Fluorescence enhancement of randomly oriented Er^{3+} near a 130 nm silver (a) or gold (b) particle. The excitation and emission wavelengths are $\lambda_{exc} = 800$ nm and $\lambda_{em} = 1.55 \mu m$, respectively. c) Extinction efficiency of a 130 nm silver (blue line) or gold (red line) particle. The embedding medium is SiO_2 (optical index $n = 1.5$).

We investigate the possibility to enhance their IR emission signal using core-shell configuration. In Erbium Doped Fiber Amplifier (EDFA), they are usually pumped at 800 or 980 nm wavelength in order to limit non radiative losses present with high energy pumping. We consider excitation wavelength $\lambda_{exc} = 800$ nm and emission at $\lambda_{em} = 1.55 \mu m$. We calculate a maximum enhancement of spherical core-shell doped with Er^{3+} for a 130 nm metal core, either for $Ag@SiO_2$ or $Au@SiO_2$. We find a maximum local enhancement up to 8.5(6.5) fold near a silver (gold) particle resulting from the excitation of the large dipolar resonance (see Fig. 6c). Our simulation gives then an average enhancement factor of 2.3 (1.7) for the whole doped volume V_0 for a silver (gold) core coated with a 25 nm doped shell layer. This poor AEF is due to the position of excitation and emission wavelength of Er^{3+} , both far from plasmon maximum. Since it is possible to red-shift the longitudinal dipolar plasmon resonance with nanoparticle presenting high aspect ratio, we propose to optimize the AEF with an elongated metal core.

3.2.2. Nanorod core-shell particle Spherical core-shell particles present limited AEF and imposes to use large particle in order to red shift the plasmon dipolar resonance to match the Er^{3+} absorption spectrum. Another possibility is to use rod shape particle with high aspect ratio [12, 41, 42]. In this last section, we investigate core-shell nanorod and estimate the fluorescent enhancement [Eqs (4) and (6)]. In this goal, the excitation electric field \mathbf{E} and emission rates Γ_i need to be evaluated at any location in the doped layer. In case of arbitrary structure, they can be calculated thanks to the Green's dyad technique [43, 44, 45]. Liaw *et al* investigate similar structures using multiple multipole

method [42]. However, they limit the computation to a plane (emitter orientation is constrained in 2 dimensions and only the doped layer inside the plane of incidence is considered). Since the highest fluorescence rate is obtained for these emitters positions and orientations, this leads to overestimate the enhancement factor of the whole doped layer. Their work however paves the way to optimize the shape of the elongated core-shell particle.

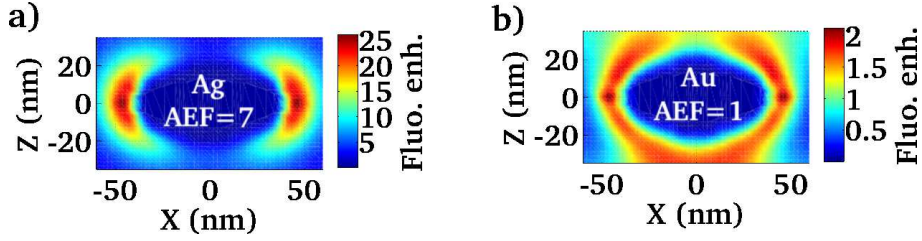


Figure 7. Fluorescence enhancement of randomly oriented Er^{3+} near a silver (a) or gold (b) nanorod ($70 \text{ nm} \times 20 \text{ nm}$). The incident electric field is polarized along the rod long axis. The excitation and emission wavelength are $\lambda_{exc} = 800 \text{ nm}$ and $\lambda_{em} = 1.55 \mu\text{m}$, respectively. The AEF over the whole (3D) 25 nm doped shell is indicated. The two first nm of the shell are undoped (SiO_2 spacer). The embedding medium is SiO_2 (optical index $n = 1.5$)

Figure 7(a) represents the fluorescent enhancement near a silver nanorod. The aspect ratio of the rod has been fixed in order to match the particle resonance and the excitation field ($\lambda_{exc} = 800 \text{ nm}$). The volume of the nanorod is the same as for a 30 nm spherical particle so that the achieved enhancement factor can be compared to the visible regime (Fig. 4a). The tip effect strengthens the field exaltation at the dipolar resonance and we observe a fluorescence enhancement up to 25 fold near the rod tip. Finally, we achieve an average enhancement factor $AEF = 7$ for the whole doped shell, comparable to the visible regime (Fig. 5). There is no improvement for a gold core ($AEF = 1$, Fig. 7b) due to high losses. Nevertheless, we would like to mention that we use the dielectric constant of bulk metal although crystalline nanoparticles present lower losses. This could lead to small improvement of the enhancement factor.

4. Conclusion

In this work, we have quantified the plasmon contribution to the luminescence enhancement of rare earth doped metallic core-shell nanoparticles. This would therefore help in discriminating and then optimizing the different enhancement mechanisms that could play a role in rare-earth doped plasmonic core-shell particles.

The highest plasmon mediated enhancement is achieved when the particle dipolar resonance matches the excitation wavelength. The enhancement mainly comes from excitation rate exaltation by coupling to the dipolar mode whereas emission process is weakly modified. It is also possible to enhance the excitation by coupling to the quadrupolar plasmon and emission by coupling to the dipolar plasmon. This offers a

supplementary degree of freedom for luminescence control. These results differ from dye-doped particles. Indeed, the small Stokes shift between emission and excitation wavelengths leads then to choose a particle resonance overlapping the two in order to enhance both excitation and radiative rates by coupling to the dipolar resonance.

We demonstrate average enhancement factor of the fluorescence on the overall RE-doped silver nanoparticle $AEF = 11$ and $AEF = 7$ in the visible and near-infrared regime, respectively. Gold core leads to lower effect due to larger losses.

These values are similar to the AEF measured on RE-metal nanocluster system [15, 27] where the enhancement originates from energy transfer. Up to 250 fold enhancement has been reported but probably due to concentration effect [27]. We however envision different applications for RE-doped core-shell plasmonic particles and RE-metal nanoclusters. Colloidal solutions of plasmonic particles can be synthesized and would benefit as *e.g* biolabels or solar cells whereas RE-nanocluster doped glasses are promising materials for telecom fiber amplification.

Acknowledgement

This work is supported by the Agence Nationale de la Recherche (Fenoptix ANR-09-NANO-23 and HYNNA ANR-10-BLAN-1016). Calculations were performed using DSI-CCUB resources (Université de Bourgogne).

- [1] D. Timmerman, I. Izeddin, P. Stallinga, I. Yassievich, T. Gregorkiewicz, Space-separated quantum cutting with silicon nanocrystals for photovoltaic applications, *Nature Photonics* 2 (2008) 105.
- [2] C. Bouzigues, T. Gacoin, A. Alexandrou, Biological Applications of Rare-Earth Based Nanoparticles, *ACS Nano* 11 (2011) 8488.
- [3] C. Wang, H. Tao, L. Cheng, Z. Liu Near-infrared light induced in vivo photodynamic therapy of cancer based on upconversion nanoparticles, *Biomaterials* 32 (2011) 6145.
- [4] J.C. Bunzli, S. Comby, A.S. Chauvin, C. Vandevyver, New Opportunities for Lanthanide Luminescence, *J. Rare Earths* 25 (2007) 257.
- [5] B. Pettinger, Single-molecule surface- and tip-enhanced Raman spectroscopy, *Molecular Physics* 108 (2010) 2039–2059.
- [6] E. Fort and S. Grésillon, Surface enhanced fluorescence, *J. Phys. D: Appl. Phys.* 41 (2008), 013001.
- [7] V. Giannini, A. I. Fernandez-Dominguez, S. C. Heck, S. A. Maier, Plasmonic nanoantennas: Fundamentals and their use in controlling the radiative properties of nanoemitters, *Chemical Reviews* 111 (2011) 3888–3912.
- [8] G. Sun, J. B. Khurgin, D. P. Tsai, Comparative analysis of photoluminescence and raman enhancement by metal nanoparticles, *Optics Letters* 37 (2012) 1583–1585.
- [9] Y. Fang, D. D. Seong, N.-H.; Dlott, Measurement of the distribution of site enhancements in surface-enhanced raman scattering, *Science* 321 (2008) 388.
- [10] P. Bharadwaj, L. Novotny, Spectral dependence of single molecule fluorescence enhancement, *Opt. Expr.* 15 (2007) 14266–14274.
- [11] C. Strohhofer, A. Polman, Silver as sensitizer for erbium, *Applied Physics Letters* 81 (2002) 1414.
- [12] H. Mertens, A. Polman, Plasmon-enhanced erbium luminescence, *Applied Physics Letters* 89 (2006) 211107.
- [13] A.C.Marques, R.M. Almeida, Er photoluminescence enhancement in Ag-doped sol-gel planar waveguides, *Journal of Non-Crystalline Solids* 353 (2007) 2613-2618.
- [14] K. Aslan, M. Wu, J. R. Lakowicz, C. D. Geddes, Fluorescent core-shell Ag@SiO₂ nanocomposites

- for metal-enhanced fluorescence and single nanoparticle sensing platforms, *J. Am. Chem. Soc.* 129 (2007) 1524–1525.
- [15] Z. Ma, D. Dosev and I. M. Kennedy, A microemulsion preparation of nanoparticles of europium in silica with luminescence enhancement using silver *Nanotechnology* 20 (2009) 085608
- [16] L. R. P. Kassab, D. S. da Silva, C. B. de Araújo, Influence of metallic nanoparticles on electric-dipole and magnetic-dipole transitions of Eu^{3+} doped germanate glasses, *Journal of Applied Physics* 107 (2010) 113506.
- [17] T. Som, B. Karmakar, Nano silver:antimony glass hybrid nanocomposites and their enhanced fluorescence application *Solid State Sciences* 13 (2011) 887–895.
- [18] J. T. van Wijngaarden, M. M. van Schooneveld, C. de Mello Donega, A. Meijerink, Enhancement of the decay rate by plasmon coupling for Eu^{3+} in an Au nanoparticle model system, *EPL* 93 (2011) 57005.
- [19] R. Reisfeld, T. Saraidarov, G. Panzer, V. Levchenko, M. Gaft, New optical material europium EDTA complex in polyvinyl pyrrolidone films with fluorescence enhanced by silver plasmons, *Optical Materials* 34 (2011) 351–354.
- [20] W. Deng, L. Sudheendra, J. Zhao, J. Fu, D. Jin, I.M. Kennedy, E.M Goldys, Upconversion in $\text{NaYF}_4:\text{Yb}$, Er nanoparticles amplified by metal nanostructures, *Nanotechnology* 22 (2011) 325604.
- [21] V.A.G. Rivera, Y. Ledemi, S.P.A. Osorio, D. Manzani, Y. Messaddeq, L.A.O. Nunes, E. Marega Jr., Efficient plasmonic coupling between $\text{Er}^{3+}:(\text{Ag}/\text{Au})$ in tellurite glasses, *Journal of non-crystalline solids* 358 (2012) 399–405.
- [22] R. Amjad, M. Sahar, M. Dousti, S. Ghoshal and M. Jamaludin, Surface enhanced Raman scattering and plasmon enhanced fluorescence in zinc-tellurite glass, *Optics Express* 21 (2013), 21282–21290.
- [23] O.L. Malta, M.A. Couto dos Santos, Theoretical analysis of the fluorescence yield of rare earth ions in glasses containing small metallic particles, *Chemical Physics Letters* 174 (1990) 13-18.
- [24] R. Esteban,1, M. Laroche and J.-J. Greffet Influence of metallic nanoparticles on upconversion processes *Journal of Applied Physics* 105 (2009), 033107
- [25] S. Fischer, F. Hallermann, T. Eichelkraut, G. von Plessen, K.W. Krämer, D. Biner, H. Steinkemper, M. Hermle, J.C. Goldschmidt, Plasmon enhanced upconversion luminescence near gold nanoparticles-simulation and analysis of the interactions, *Optics Express* (2012) 271-282.
- [26] S. Karaveli, R. Zia, Spectral Tuning by Selective Enhancement of Electric and Magnetic Dipole Emission *Physical Review Letters* 106 (2011) 193004
- [27] M. Eichelbaum, K. Rademann, Plasmonic enhancement or energy transfer? on the luminescence of gold-, silver-, and lanthanide-doped silicate glasses and its potential for light-emitting devices, *Advanced Functional Materials* 19 (2009) 2045–2052.
- [28] M. Busson, B. Rolly, B. Stout, J. W. N. Bonod, S. Bidault, Photonic engineering of hybrid metal-organic chromophores, *Angew. Chem. Int. Ed.* 51 (2012) 11083–11087.
- [29] C. Maurizio, E. Trave, G. Perotto, V. Bello, D. Pasqualini, P. Mazzoldi, G. Battaglin, T. Cesca, C. Scian, G. Mattei, Enhancement of the Er^{3+} luminescence in Er-doped silica by few-atom metal aggregates, *Physical Review B* 83 (2011) 195430.
- [30] B. Peng, Q. Zhang, X. Liu, Y. Ji, H. Demir, C. Huan, T. Sum and Q. Xiong, Fluorophore-Doped Core Multishell Spherical Plasmonic Nanocavities: Resonant Energy Transfer toward a Loss Compensation, *ACS Nano* 6 (2012), 6250–6259.
- [31] J.-W. Liaw, C.-L. Liu, W.-M. Tu, C.-S. Sun, M.-K. Kuo, Average enhancement factor of molecules-doped coreshell ($\text{Ag}@\text{SiO}_2$) on fluorescence, *Optics Express* 18 (2010) 12788–12797.
- [32] P. Johnson, R. Christy, Optical constants of the noble metals, *Physical Review B* 6 (1972) 4370–4379.
- [33] G. Colas des Francs, A. Bouhelier, E. Finot, J.-C. Weeber, A. Dereux, C. Girard, E. Dujardin, Fluorescence relaxation in the near-field of a mesoscopic metallic particle: distance dependence and role of plasmon modes, *Optics Express* 16 (2008) 17654–17666.

- [34] G. Colas des Francs, C. Girard, A. Dereux, Theory of near-field optical imaging with a single molecule as a light source, *Journal of Chemical Physics* 117 (2002) 4659–4666.
- [35] G. Lévêque *et al.* Polarization state of the optical near-field, *Physical Review E* 65 (2002), 36701.
- [36] Y. S. Kim, P. T. Leung, T. F. George, Classical decay rates for molecules in the presence of a spherical surface: a complete treatment, *Surface Science* 195 (1988) 1–14.
- [37] J. Sinzig, M. Quinten, Scattering and absorption by spherical multilayer particles, *Applied Physics A* 58 (1994) 157–162.
- [38] V. Reineck, D. Gómez, S. Ng, M. Karg, T. Bell, P. Mulvaney and U. Bach, Distance and Wavelength Dependent Quenching of Molecular Fluorescence by Au@SiO₂ Core-Shell Nanoparticles, *ACS Nano* 7 (2013) 6636.
- [39] T. Härtling, P. Reichenbach, L. M. Eng, Near-field coupling of a single fluorescent molecule and a spherical gold nanoparticle, *Optics Express* 15 (2007) 12806–12817.
- [40] A. Pillonnet, A. Berthelot, A. Pereira, O. Benamara, S. Derom, G. Colas des Francs, A.-M. Jurduc, Coupling distance between Eu³⁺ emitters and Ag nanoparticles, *Applied Physics Letters* 100 (2012) 153115.
- [41] H. Mertens, A. Polman, Strong luminescence quantum-efficiency enhancement near prolate metal nanoparticles: Dipolar versus higher-order modes, *Journal of applied physics* 105 (2009) 44302.
- [42] J.-W. Liaw, H.-Y. Tsai, Theoretical investigation of plasmonic enhancement of silica-coated gold nanorod on molecular fluorescence, *Journal of Quantitative Spectroscopy and Radiative Transfer* 113 (2012) 470–479.
- [43] C. Girard, Near-field in nanostructures, *Report on Progress in Physics* 68 (2005) 1883–1933.
- [44] G. Baffou, C. Girard, E. Dujardin, G. Colas des Francs, O. Martin, Molecular quenching and relaxation in a plasmonic tunable nanogap, *Physical Review B* 77 (2008) 121101(R).
- [45] C. Girard, E. Dujardin, G. Baffou, R. Quidant, Shaping and manipulation of light fields with bottom-up plasmonic structures, *New Journal of Physics* 10 (2008) 105016.